Available online at www.sciencedirect.com
SCIENCE DIRECT®
Journal of Molecular Graphics and Modelling 22 (2004) 293–307
Journal of Molecular Graphics and Modelling
www.elsevier.com/locate/JMGM

A practical approach to docking of zinc metalloproteinase inhibitors

Xin Hu, Stefan Balaz, William H. Shelver*

Department of Pharmaceutical Science and the Center for Protease Research, North Dakota State University, Fargo, ND 58105, USA

Accepted 13 November 2003

Abstract

Forty zinc-dependent metalloproteinase/ligand complexes with known crystal structures were re-docked using five docking/scoring approaches (DOCK, FlexX, DrugScore, GOLD, and AutoDock). Correct geometry of the coordination bonds between the ligand's zinc binding group (ZBG) and the catalytic zinc is important for docking accuracy and scoring reliability. More than 75% of docked poses with RMSD less than 2 Å were found to have appropriate ZBG binding, but for poor ZBG binding, about 95% of poses failed to dock correctly. Elimination of poses with inappropriate zinc binding resulted in better binding energy predictions that were further improved by dividing the ligands into subsets according to the ZBG (carboxylates, hydroxamates, and phosphorus containing groups). After a subset re-scoring using the regression functions obtained for individual subsets, DrugScore was able to explain 77% and the consensus scoring scheme X-CSCORE even 88% of variance in binding energies. The approach combining ZBG-based pose selection and subset re-scoring improved the hit rate in virtual screening for metalloproteinase inhibitors for all tested methods by 4–16%.
© 2003 Elsevier Inc. All rights reserved.

Keywords: Metalloproteinases; Zinc binding group (ZBG); Comparative docking; Consensus scoring; Virtual screening

1. Introduction

Docking as an efficient *in silico* screening tool is playing an ever-increasing role in rational drug design [1,2]. In the past decade, a number of docking approaches have been developed to improve the docking accuracy and scoring reliability, the two fundamental aspects by which docking programs are assessed [3]. Docking accuracy refers to finding the binding mode of a ligand matching closely the experimental conformation with the lowest energy among a large sampling of potential docking solutions. Scoring reliability, on the other hand, can be defined as the ability to correctly rank ligands based on their predicted binding affinities, allowing the docking system to extract a small number of tightly binding ligands from a large database [4]. Docking accuracy and scoring reliability are directly associated with two interrelated issues in the docking process: the searching algorithm and the scoring function. Various searching algorithms, such as fast shape matching [5,6], simulated annealing [7], incremental construction [8,9], genetic algorithms [10–12], Monte Carlo [13], and Tabu search [14], have been utilized in docking programs. The algorithms differ in the area covered, randomness, and speed, but all perform rather well when tested against complexes of known structure. In contrast, scoring functions, which are commonly categorized as force field-based methods [5,12], empirical free energy scoring functions [8,11,15–17], and knowledge-based scoring functions [18–20], are only marginally successful. Due to the inadequate descriptions of the complex molecular interactions involved in the receptor-ligand binding and the need for speed in docking, these scoring approaches are approximate. Consequently, a great deal of research has focused on the improvement of prediction of binding affinities [21,22].

Metalloproteinases represent a class of zinc-dependent endopeptidases that selectively catalyze hydrolysis of the polypeptide bond [23]. As promising therapeutic drug targets, zinc metalloproteinases have recently attracted great interest in the search of potent and selective inhibitors using computer-aided molecular modeling and docking techniques [24–28]. However, modeling of ligand binding to zinc ion is quite problematic due to multiple coordination geometries and the lack of force fields capable of reproducing these phenomena [29]. Ligand/metal interactions in docking studies remain a challenge despite intense investigation [30–33]. In connection with our efforts in virtual screening for novel inhibitors of metalloproteinases such as matrix metalloprotienases (MMPs) [34] and tumor necrosis factor α-converting enzyme (TACE) [35], we performed a comparative docking study with four widely used programs:

* Corresponding author. Tel.: +1-701-232-3071.
E-mail address: william.shelver@ndsu.nodak.edu (W.H. Shelver).

1093-3263/$ – see front matter © 2003 Elsevier Inc. All rights reserved.
doi:10.1016/j.jmgm.2003.11.002

DOCK [6], FlexX [8], AutoDock [11], and GOLD [12]. The docking accuracy and scoring reliability of the docking approaches were evaluated by docking 40 metalloproteinase ligands with known crystal structures and correlating the predicted binding affinities with the experimental values. The problems associated with ZBG geometry were analyzed, and an improved solution for virtual screening of metalloproteinase inhibitors was proposed.

2. Methods

2.1. Zinc metalloprotein/ligand complexes

X-ray crystal structures of metalloproteinases were obtained from the Protein Data Bank (PDB) [36]. The complexes were selected based on the following criteria: (1) crystal structures with resolution better than 2.5 Å, (2) temperature factor of zinc lower than 20, (3) the dissociation constant (K_i) of the complex available. In addition, the structural and functional diversities of both metalloproteinases and ligands were considered. Table 1 lists the selected 40 metalloproteinase/ligand crystal structures (20 matrix metalloproteinases, 13 thermolysins, and 7 carboxypeptidases). The ligands (Fig. 1) contain all common zinc binding groups (ZBG): hydroxamate, carboxylate, phosphate, phosphonate, phosphoramidate, sulfonamide, thiolate, and thiadiazole. The flexibility of the ligands varies from 4 to 18 rotatable bonds.

The Sybyl 6.8 package [56] was used to prepare the protein and ligand data required in docking. The ligand was extracted from the complex, hydrogen atoms were added, and partial charges were assigned to the atoms according to the method of Gasteiger and Marsili [57]. A short minimization (100 steepest descent steps with Tripos force field) was performed to release internal strain. All ligands were used in deprotonated forms with negatively charged ZBG. For hydroxamates that exist in a number of different tautomeric forms, the one in agreement with FlexX was selected [8]. The hetero atoms including cofactors, water molecules, and the ligand were removed from the protein except for the zinc ion in the active site. As special cases, the water molecules in 3TMN and 2CTC, which mediate the binding between zinc and the ligand, were also retained. Hydrogen atoms were assigned with either all-atom or united atom model. The protonation states of histidines and glutamates in the binding site of metalloproteinases are listed in Table 2.

2.2. Docking

Four docking programs, DOCK 4.0, FlexX 1.10, GOLD 1.2, and AutoDock 3.0, were used in this study. The scoring function DrugScore with FlexX as the searching engine was evaluated as a separate approach. In general, the default settings for virtual screening were adopted. Docking was carried out on a dual-CPU SGI workstation (Sybyl/FlexX package, GOLD 1.2) and a Linux system with dual-CPU PIII 800 (AutoDock 3.0, DOCK 4.0). The time for an individual docking was approximately 1–2 min for DOCK, FlexX, DrugScore, and GOLD, and 2–5 min for AutoDock.

2.2.1. DOCK 4.0

DOCK uses fast shape matching to search the sampling space and a grid-based energy calculation for fast evalua-

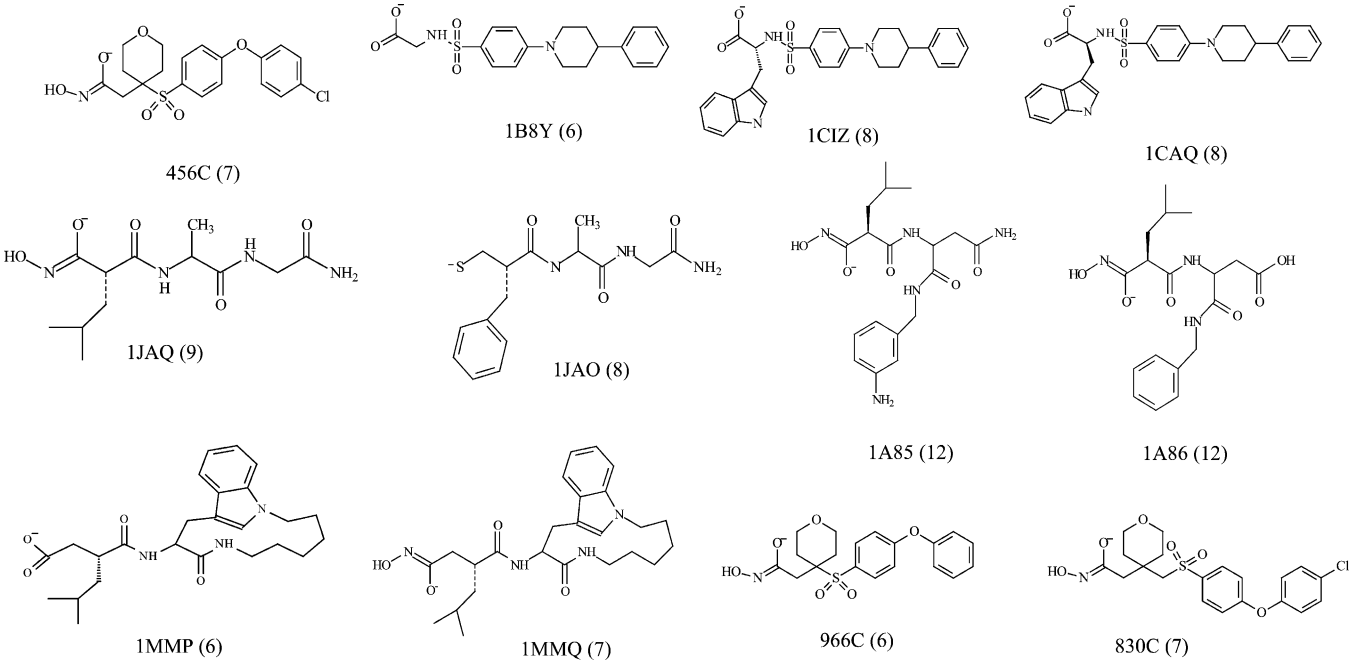

Fig. 1. Structures of ligands in metalloproteinase complexes. The number of rotatable bond is given in parentheses.

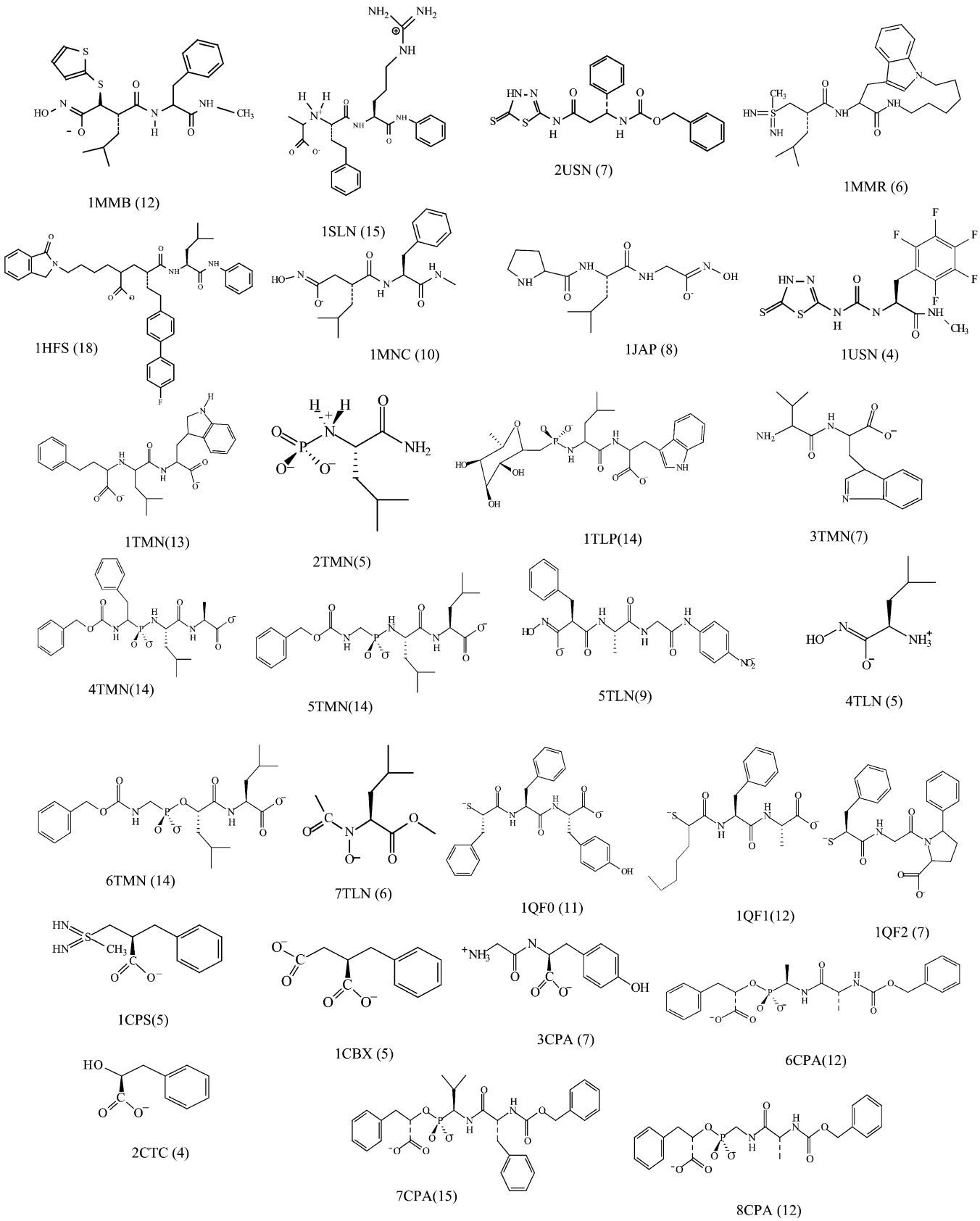

Fig. 1. (*Continued*).

Table 1
Structure of metalloproteinase complexes used in this study

PDB	Protein	Ligand	Ligand type	Resolution (Å)	pK_i	B (Zn)	Geometry[a]	Distance[b] (Å)		RMSD[c]	Ref.
966C	MMP-1	RS2	Hydroxamate	1.90	7.64	5.77	SP	2.10	2.21	21.79	[37]
456C	MMP-13	RS-112356	Hydroxamate	2.40	9.77	15.22	SP	1.89	1.96	17.86	[37]
830C	MMP-13	RS-130830	Hydroxamate	1.60	9.28	11.06	SP	2.04	1.85	17.35	[37]
1CAQ	MMP-3	DPS	Carboxylate	1.64	7.44	14.87	TB	1.99	2.83	18.28	[38]
1CIZ	MMP-3	DPS	Carboxylate	1.80	7.72	10.49	TB	2.09	2.62	17.69	[38]
1B8Y	MMP-3	IN7	Carboxylate	2.00	7.85	19.53	TB	2.02	2.85	18.55	[38]
1SLN	MMP-3	INH	Carboxylate	2.27	6.64	9.21	TB	1.75	3.00	26.61	[39]
1HFS	MMP-3	L04	Carboxylate	1.70	8.70	13.92	TB	1.84	2.62	16.40	[40]
2USN	MMP-3	PNU-141803	Thiadiazole	2.20	6.51	8.62	TH	2.28	–	9.99	[41]
1USN	MMP-3	PNU-142372	Thiadiazole	1.80	7.74	12.74	TH	2.39	–	10.42	[41]
1MMQ	MMP-7	RRS	Hydroxamate	1.90	7.52	14.51	SP	2.16	2.20	18.18	[42]
1MMP	MMP-7	RSS	Carboxylate	2.30	6.07	14.21	TB	1.96	2.66	19.64	[42]
1MMR	MMP-7	SRS	Sulfodiimine	2.30	5.40	13.27	TH	2.00	–	13.80	[42]
1MMB	MMP-8	Batimastat	Hydroxamate	2.10	9.22	21.01	TB	2.00	2.69	17.12	[43]
1JAO	MMP-8	BTP-Asp-GM1	Thiolate	2.40	5.92	9.37	TH	2.24	–	11.07	[44]
1JAQ	MMP-8	HMP-Asp-GM1	Hydroxamate	2.25	4.48	10.04	TB	2.45	2.10	17.41	[44]
1A85	MMP-8	HMI-Asn-BNN	Hydroxamate	1.80	7.59	8.06	TB	2.35	2.16	15.17	[45]
1A86	MMP-8	HMI-Asp-BNN	Hydroxamate	1.90	6.87	10.11	TB	1.87	2.41	15.60	[45]
1MNC	MMP-8	PLH	Hydroxamate	2.10	9.00	10.13	TB	2.11	2.29	17.73	[46]
1JAP	MMP-8	ProLeuGly-NHOH	Hydroxamate	2.50	4.72	16.64	SP	2.18	1.91	15.20	[47]
1TLP	Thermolysin	Phosphorarnidon	Phosphoramidate	2.30	7.56	8.45	OH	1.75	–	34.27	[48]
1TMN	Thermolysin	CLT	Carboxylate	1.90	7.47	14.25	TB	2.01	2.41	17.54	[48]
2TMN	Thermolysin	*N*-phosphory-L-leucinarnide	Phosphoramidate	1.60	5.89	11.82	TB	2.06	2.79	22.10	[48]
3TMN	Thermolysin	ValTrp	Amide	1.70	5.90	17.30	TH	2.13		13.79	[48]
4TMN	Thermolysin	ZFPLA	Phosphinate	1.70	10.17	12.29	OH	2.17	2.59	31.74	[48]
4TMN	Thermolysin	Leu-NHOH	Hydroxamate	2.30	3.72	14.37	TB	2.00	2.10	22.36	[48]
5TMN	Thermolysin	ZGP(NH)LL	Phosphinate	1.60	8.04	9.54	TB	2.08	3.00	21.36	[48]
5TLN	Thermolysin	INA	Hydroxamate	2.30	6.37	16.69	TB	2.10	2.26	21.47	[48]
6TMN	Thermolysin	ZGP(O)LL	Phosphonate	1.60	5.05	10.83	TB	2.07	2.98	20.76	[48]
7TLN	Thermolysin	CH_2CO-Leu-OCH_3	Hydroxamate	2.30	2.47	17.10	TB	2.48	2.85	19.34	[48]
1QF0	Thermolysin	(2-Sulfanyl-3-phenylpropanoyl)-FY	Thiolate	2.20	7.38	6.08	TH	2.38	–	13.38	[49]
1QF1	Thermolysin	2-Sulfanyiheptanoyl-FA	Thiolate	2.00	7.32	6.80	TH	2.29	–	14.82	[49]
1QF2	Thermolysin	(2-Sulfanyl-3-phenylpropanoyl)-G-(5-phenylproline)	Thiolate	2.06	5.92	7.39	TH	2.29	11.85	–	[49]
1CBX	Carboxypepfidase A	Benzylsuccinate	Carboxylate	2.00	6.30	5.61	011	2.30	2.30	34.42	[50]
1CPS	Carboxypeptidase A	Sulfodiimide	Sulfodiimine	2.25	6.66	4.85	SP	2.24	–	14.03	[51]
2CTC	Carboxypeptidase A	Phenyllactate	Carboxylate	1.40	3.89	8.86	TB	2.00	–	16.36	[52]
3CPA	Carboxypeptidase A	GT	Amide	2.00	3.88	10.00	SP	2.78	2.93	17.40	[53]
6CPA	Carboxypeptidase A	ZAAP(O)F	Phosphonate	2.00	11.52	9.00	TB	2.15	3.07	20.66	[54]
7CPA	Carboxypeptidase A	BZ-FVP(O)F	Phosphonate	2.00	14.0	10.29	TB	2.19	2.98	19.23	[55]
8CPA	Carboxypeptidase A	BZ-AGP(O)F	Phosphonate	2.00	9.15	8.70	TB	1.88	3.09	22.28	[55]

[a] Geometry: TB-trigonal bipyramidal, SP-square-based pyramidal, TH-tetrahedral, OH-octahedral.

[b] Distances are measured between zinc and coordinated atoms of ligand.

[c] The geometry fit was measured by root-mean-square deviation of angles, RMSD $= [\sum(\alpha_i - \alpha_{\text{ideal}})^2/n]^{1/2}$, where α_i is the measured angle (L-Zn-L), α_{ideal} is the angle in ideal coordination geometry, and n is the total number of angles of the corresponding geometry (6-TH, 10-TB/SP, and 15-OH).

Table 2
Protonation and tautomeric states of histidines and glutamates in the binding sites

Metalloproteinases	Residues at zinc binding site	Protonation form
Matrix metalloproteinase	His201	Neutral (H on δ-N)
	His205	Neutral (H on δ-N)
	His211	Neutral (H on δ-N)
	Glu202	Neutral (H on OE2)
Thermolysin	His142	Neutral (H on δ-N)
	His146	Neutral (H on δ-N)
	Glu166	Charged
	Glul43	Neutral (H on OE2)
Carboxypeptidase A	His69	Neutral (H on ε-N)
	His196	Neutral (H on ε-N)
	Glu72	Charged
	Glu270	Neutral (H on OE2)

tion [6]. DOCK 4.0 offers several scoring functions including contact scoring, chemical scoring, and energy scoring. The energy scoring function consists of a Coulombic electrostatic potential and a Lennard–Jones 12–6 potential term. The metal/ligand interactions are modeled using electrostatic interactions and van der Waals potentials.

The protein active site was defined as a 6.5 Å radius sphere centered at the center of mass of the ligand. A Connolly surface was generated at the active site by using the MS program [58], with the parameters of 1.4 Å probe radius and 5.0 surface points per $Å^2$. Sphere clusters were visually inspected; the best one with 40–50 spheres on average was used to construct the grid box. The grid with a spacing of 0.375 Å was constructed around the active site. The grid encloses the spheres to be used for docking, along with an extra margin of 6 Å. Energy scoring grids were computed by using an all-atom model, 6–12 Lennard–Jones potential, and the distance-dependent dielectric function of $4r$ with a 10 Å cut-off. All-atom model with Amber95 atomic charges was used. Since zinc parameters were not available in DOCK, the vdW parameters $r = 1.1$ Å, $\varepsilon = 0.25$ kca1/mol, and the formal charge of +2e were used.

A completely flexible docking with subsequent minimization was performed with automatic matching of an anchor fragment within a maximum of 500 orientations. Energy scoring was calculated for each orientation without intramolecular interactions. One hundred cycles of 250 simplex minimization steps were performed to a convergence of 0.1 kca1/mol. The top 30 solutions were ranked according to the energy scores. RMSD was computed between docking conformations and the experimental conformation in crystal structure.

2.2.2. FlexX 1.10

FlexX uses a pure empirical scoring function similar to that developed by Böhm and coworkers [8,15]. The free binding energy of a protein/ligand complex is estimated as the sum of free energy contributions from hydrogen bonding, ion-pair interactions, hydrophobic and π-stacking interactions of aromatic groups, and lipophilic interactions. A scaling function is used to penalize deviations from ideal geometry. Metal/ligand interaction is treated as an ionic interaction. FlexX is also used with a knowledge-based scoring function DrugScore. Its interactive potentials are based on statistical preferences for interatomic distances obtained by detailed analysis of high quality ligand-receptor X-ray structures from the PDB [19].

Standard docking conditions of the FlexX program were adopted as implemented in the 6.8 release of the Sybyl package. Generally, a receptor description file was defined from the PDB coordinates through the FlexX graphic interface, and zinc ion at the active site was added. The active site includes protein residues in a 6.5 Å radius sphere centered on the center of mass of the ligand. Formal charges were assigned for the ligand. For each docking with different scoring functions (the original FlexX scoring function and DrugScore), the top 30 solutions were saved.

2.2.3. GOLD 1.2

GOLD uses a genetic algorithm to explore the full range of ligand conformational flexibility with partial flexibility of the protein [12]. The GOLD scoring function includes the terms for hydrogen-bonding, vdW, and intramolecular energies. The vdW interactions for the protein/ligand complex are described by a 8–4 potential. A 12–6 potential is used for the ligand steric energies that also include the torsional energies. Two geometrical models for zinc coordination (tetrahedral and octahedral) are implemented in GOLD. The metal/ligand interactions are modeled in a similar fashion as hydrogen bonding.

The active site with a 10 Å radius sphere was defined in a similar way as in DOCK and FlexX. For each independent genetic algorithm (GA) run, a maximum number of 1000 GA operations was performed on a single population of 50 individuals. Operator weights for crossover, mutation, and migration were set to 100, 100, and 0, respectively. To allow poor nonbonded contacts at the start of each GA run, the maximum distance between hydrogen donors and fitting points was set to 5 Å, and nonbonded vdW energies were cut-off at 10 Å. The "early-termination" option was not selected, and a set of 30 solutions for each ligand was saved.

2.2.4. AutoDock 3.0

AutoDock 3.0 uses a force field-based empirical free energy scoring function [11]. The first three terms are a subset of AMBER potential energies, including Lennard–Jones 12–6 dispersion/repulsion interactions, the directional 12–10 hydrogen bonding interactions, and the Coulombic electrostatic potential. The remaining energy terms are measures of the unfavorable entropy of ligand binding due to the restriction of conformational degree of freedom and the desolvation effects. The desolvation parameter was assigned to protein using ADDSOL modules of AutoDock.

As in DOCK, the zinc parameters were set as $r = 1.1$ Å, $\varepsilon = 0.25$ kca1/mol, and the formal charge of +2e.

The Lamarckian genetic algorithm (LGA) was used as a search engine. The active site was defined using AutoGrid. The grid size was set to 70 × 70 × 70 points with a grid spacing of 0.375 Å centered on the mass of original ligand in the crystal structure complex. Step sizes of 1 Å for translation and 50 for rotation were chosen, a maximum number of energy evaluations was set to 250,000. For each of the 30 independent runs, a maximum number of 27,000 LGA operations was generated on a single population of 50 individuals. Operator weights for crossover, mutation, and elitism were set to 0.80, 0.02, and 1, respectively.

2.3. Virtual screening

A focused MMP inhibitor library was built to test the performance in virtual screening. A set of 490 compounds was selected from the NCI database (supplied by Tripos with UNITY 4.3) using ZBGs (hydroxamate, carboxylate, and phosphonate) as the preliminary filter. The molecular weight varied from 200 to 500. All compounds were transformed into a Sybyl database. Three-dimensional coordinates were generated using the CONCORD program. The ZBG was set in the ionized form, and the Gasteiger–Marsili charges were assigned. In the last step, 10 MMP inhibitors (4 hydroxamates, 3 carboxylates, and 3 phosphonates) were added to the library. The potencies (K_i) of these MMP inhibitors range from 1 to 500 nM.

3. Results and discussion

3.1. Overall assessment of docking accuracy

Forty ligand/metalloproteinase complexes (Table 1) were docked using five docking approaches with 30 runs for each approach. The well-docked complexes (RMSD < 2.0 Å) in the top-ranked poses (lowest docked energy) were enumerated. We also identified the best pose (the one with the lowest RMSD) and tabulated the number of well-docked poses. Finally, we identified the poses in which the ZBG group showed proper geometry (the criteria are given in part Assessment of ZBG binding) and counted those well-docked. The results of the three pose selections are summarized in Table 3.

The ability to find a well-docked complex as the top-ranked pose is crucial for docking programs. Table 3 shows that GOLD performed best with 21 well-docked poses in the top rank. In Fig. 2, the ascendingly sorted RMSD values of the first ranked poses are plotted versus the rank number, providing an illustration of the docking accuracy of the different approaches on the metalloproteinases. The superiority of GOLD and AutoDock is clearly visible. For the five docking approaches, the fraction of the well-docked poses in the top rank is only about half to two-thirds of the best poses among the 30 solutions. More than 30% of the well-docked poses are not ranked on the top. This kind of hard failure reveals the inaccuracy of scoring function implemented in each program [59]. DrugScore is the most robust in this aspect, giving 70% of well-docked poses in top rank to the best poses.

Table 3
The number of well-docked cases (RMSD < 2 Å) for 40 metalloproteinase complexes obtained by the different docking approaches

Pose	DOCK	FlexX	DrugScore	GOLD	AutoDock
Top ranked[a]	8	14	16	21	16
Best[b]	15	21	22	30	28
ZBG-selected[c]	13	17	18	25	24

[a] Complex with the lowest energy.
[b] Complex with the lowest RMSD.
[c] Top-ranked complex with good/fair ZBG geometry among 30 docked poses.

The best pose (lowest RMSD) found within the 30 solutions provides an indication of whether the experimental structure is found by the docking program regardless of its energy. The results showed relatively poor performance ranging from 38 to 75%. These rates were surprisingly low, indicating the docking programs often failed to find the correct binding mode. Among the best results, GOLD had 75% that were well-docked, while AutoDock had 65%. Both GOLD and AutoDock use genetic algorithms, which seem to be more efficient than other search methods.

The complexity of the ligands has a great effect on the docking accuracy. As shown in Table 4, almost all the well-docked solutions in the top-ranked poses are found for ligands with less than 10 rotatable bonds. For highly flexible ligands with more than 10 rotatable bonds, the docking procedures usually failed.

Evaluation of docking accuracy of docking programs requires the programs run at approximately compara-

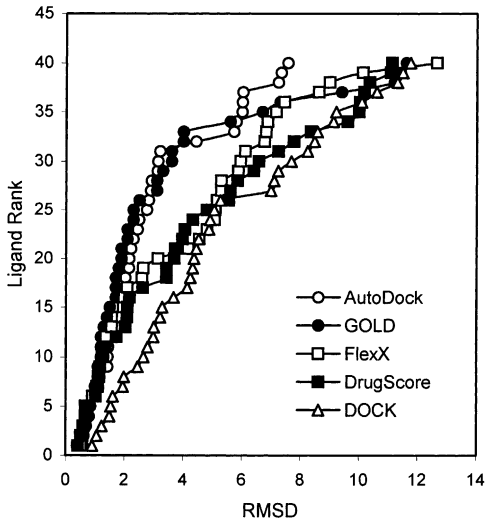

Fig. 2. RMSD of the top-ranked poses as a function of ligand rank for the five docking/scoring approaches.

Table 4
Docking accuracy as a function of the number of rotatable bond of ligand

No. of rotatable bond	No. of ligands	Well-docked (RMSD < 2 Å) top poses				
		DOCK	FlexX	DrugScore	GOLD	AutoDock
4–5	6	3	3	5	6	4
6	5	3	4	4	5	3
7	7	1	3	3	4	4
8	4	0	2	2	4	2
9	2	0	0	1	0	1
10–11	2	1	0	0	1	0
12	6	0	1	1	1	2
13–14	5	0	1	0	0	0
>15	3	0	0	0	0	0

ble speeds. Improvement of docking accuracy with increased computational time varies for different docking programs and is difficult to assess. AutoDock is more reliable and robust in achieving highly accurate docking results; however, it is also the most time-consuming approach. DOCK uses a fast shape-matching searching method, providing the advantage of high speed necessary for virtual screening of large databases. Optimization of methodology for each docking program could improve the performance and might give a different comparative rank.

3.2. Docking problems associated with zinc

A number of docking results were found to have incorrect zinc binding. Fig. 3a shows the superimposed structures of the ligand in 3CPA and docked poses by each docking approach. The lowest energy conformations predicted by Gold and DrugScore had a proper ZBG binding with the amide bound to Zn and the carboxylic acid forming a hydrogen bond with Arg145. However, for DOCK, FlexX, and AutoDock, the carboxylate group rather than the amide bound to zinc, resulting in large RMSD values. Dockings of 1HFS (Fig. 3b) resulted in RMSD > 2.0 Å for all five approaches. DOCK, GOLD, and DrugScore produced significant differences between the docked pose and crystal structure with RMSD values greater than eight and improper ZBG binding. In contrast, AutoDock and FlexX gave better results with an RMSD of 2.91 Å, and 2.63 Å and a proper ZBG binding.

The problem in the 3CPA docking using AutoDock and DOCK probably arose from the high electrostatic interactions between the positive-charged zinc ion and negative-charged carboxylate group. The use of the charge of +2e on zinc may not be realistic since the charge is actually delocalized on the coordinating atoms. As a result of the use of full charge on zinc, the energy of zinc/ligand binding would be overestimated due to the strong electrostatic interactions. Docking of 1HFS ligand is a challenge due to the high ligand flexibility. However, when constraints are put between zinc and ZBG, the correct binding mode can be predicted easily, indicating the ZBG binding is one of the primary determinants for proper docking.

The metal-related problems in docking are further complicated by the difficulty to reproduce the multiple coordination geometries of zinc complex. As shown in Fig. 4a, the bidentate binding of carboxylate to zinc was not reproduced in the 1 CIZ docking by AutoDock: only one oxygen of carboxylate bound to zinc, and the other oxygen pointed to the opposite direction. A similar result was observed in the case of 830C docking using FlexX: only monodentate binding geometry was predicted for the hydroxamate ligand (Fig. 4b).

3.3. Assessment of ZBG binding

Based on the fact that the ZBG binding dominates interactions of ligands with metalloproteinases, we have evaluated the docking quality of ZBG binding in the 40 metalloproteinases for each docking program. A variety of zinc coordination geometries exist in protein/ligand complexes [60]. Thiolate and sulfonamides are typically coordinated to zinc with a tetrahedral geometry. Hydroxamate, carboxylate, phosphonate, and phosphinate adopt a bidentate mode with distorted trigonal bipyramidal coordination geometry. Square-based pyramidal and octahedral geometries are also observed. The multiple zinc coordination geometries play a critical role in the stability of the metalloproteinase inhibitor complex [61]. Fig. 5 shows the zinc coordination with three common ZBGs found in metalloproteinases. For each ZBG type, the bond distances are quite uniform, indicating a standard geometry.

To assess the ZBG binding, we use the distances between zinc and the ligating atoms as a primary measure of a bond between zinc and the docked ligand. The overall geometry fit is measured using the root mean square deviation (RMSD) of the angles between docked and ideal geometries. The ideal values of distances and RMSD for the 40 crystal structures of metalloproteinase ligand complexes are listed in Table 1. Table 5 shows a classification scheme for the ZBG binding. The ZBG binding is considered good if both distance and angles fit well, and fair if the distance is within the reasonable

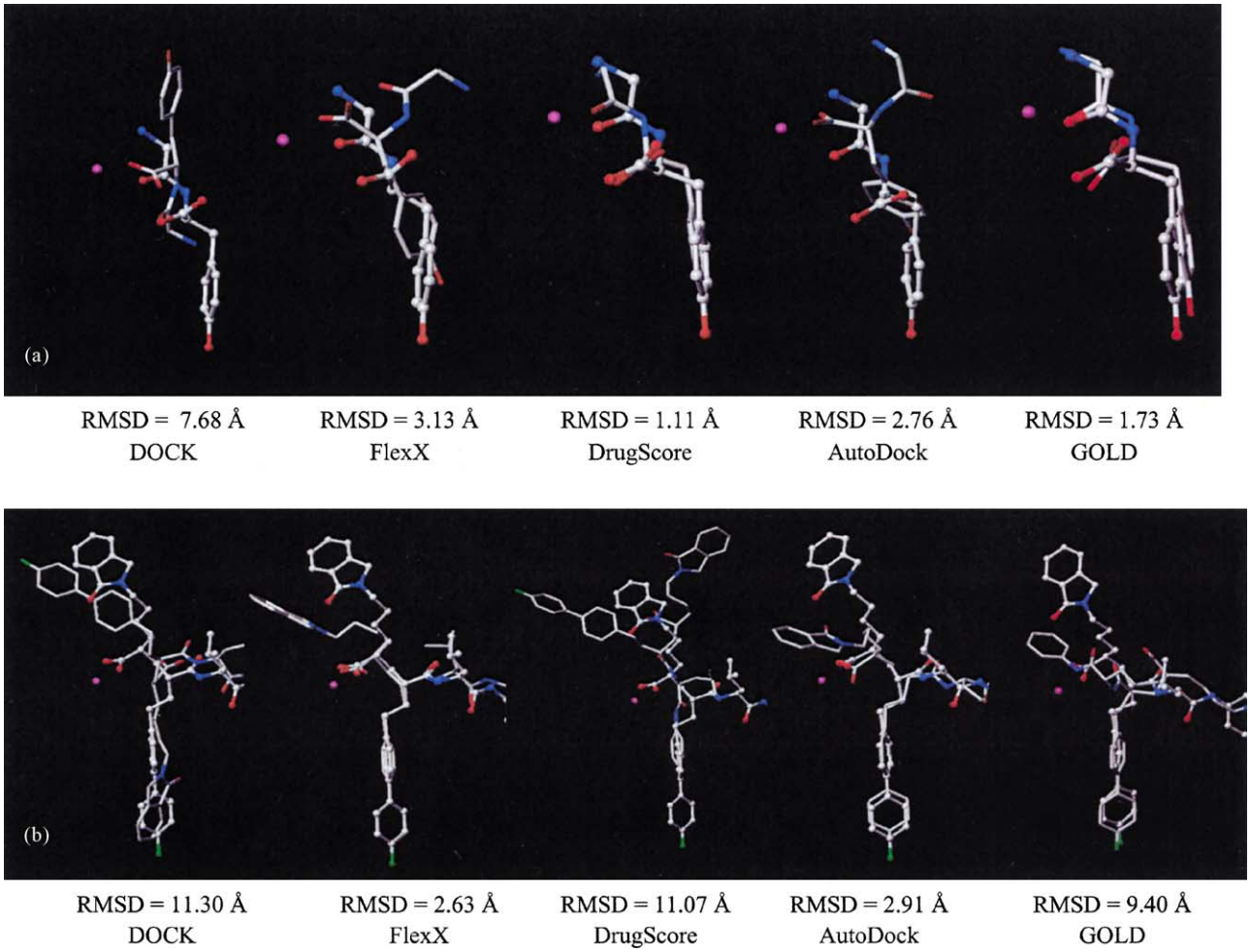

Fig. 3. Examples of docking results for (a) 3CPA and (b) 1HFS generated by the five docking/scoring approaches. The RMSD is given below the structures. The balls and sticks represent the experimental conformation, and the sticks represent the docked conformation.

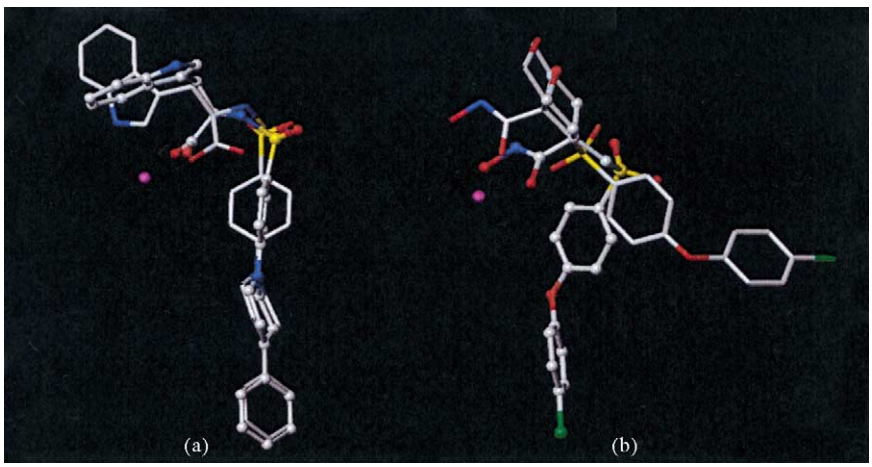

Fig. 4. Examples of docking results: (a) 1CIZ/AutoDock, RMSD = 1.87 Å and (b) 830C/FlexX, RMSD = 5.28 Å. The balls and sticks represent the experimental conformation, and the sticks represent the docked conformation.

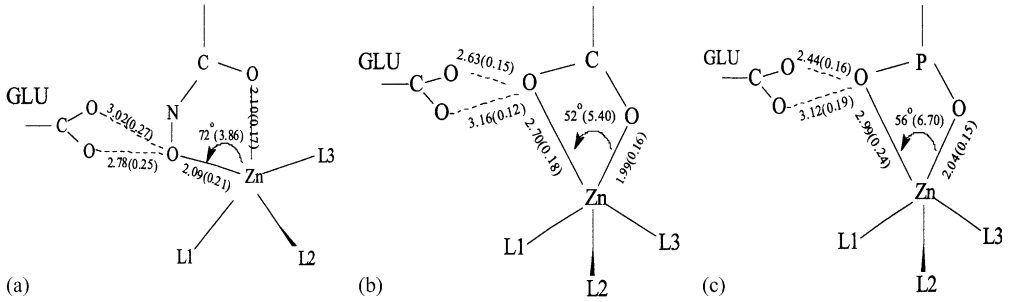

Fig. 5. Experimental binding geometries of (a) hydroxamates, (b) carboxylates, and (c) phosphonates (phosphinate, phosphoramidates) in metalloproteinases. L1, L2, and L3 represent either histidine or glutamic acid residues. Bond lengths and angles represent average values for all studied complexes (Table 1). Standard deviations are given in the parentheses (13 hydroxamates, 8 carboxylates, and 8 phosphonates (phosphinate, phosphoramidates)).

Table 5
Criteria for evaluation of the docking accuracy of ZBG binding

	Rating		
	Good	Fair	Poor
Distance (Å)[a]	<3.0	<3.0	>3.0
Geometry (RMSD)[b]			
Tetrahedral	<15	>15	>15
Trigonal bipyramidal	<25	>25	>25
Square-based pyramidal	<25	>25	>25
Octahedral	<35	>35	>35

[a] A distance of 3.0 Å is selected to indicate coordination with the zinc atom. The cut-off is the largest distance found in the experimental structures.

[b] RMSD based on the difference between the docked and experimental structure of the angles that defines the geometry of the zinc coordination. The cut-off of each geometry is the largest RMSD found in the experimental structures.

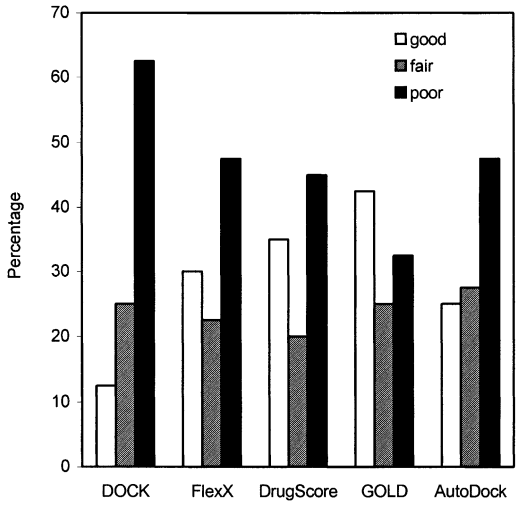

Fig. 7. Geometry of ZBG binding for top poses. The classification criteria are given in Table 5.

range but the angular fit fails. Fig. 6 illustrates the three categories of ZBG binding quality.

The docking accuracy of ZBG in the top-ranked poses predicted by each docking approach is summarized in Fig. 7. Good ZBG binding was observed with 12, 30, 35, 42, and 25% of the cases for DOCK, FlexX, DrugScore, GOLD, and AutoDock, respectively. Such a poor docking accuracy with respect to the ZBG binding indicated that inability to handle the zinc coordination properly is common to most docking programs. Among the five docking approaches, GOLD was shown to be superior to others. Out of 40 complexes, 17 top poses were docked with good ZBG binding, and 10 top poses were fair. Totally, about 70% of dockings by GOLD had a good/fair ZBG binding. On the other hand, DOCK

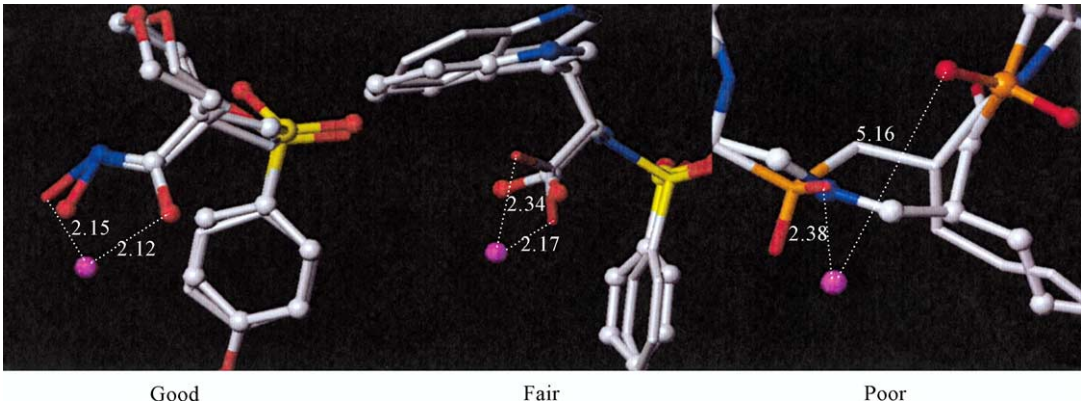

Fig. 6. An illustration of docking accuracy at the zinc binding site. The criteria are described in Table 5.

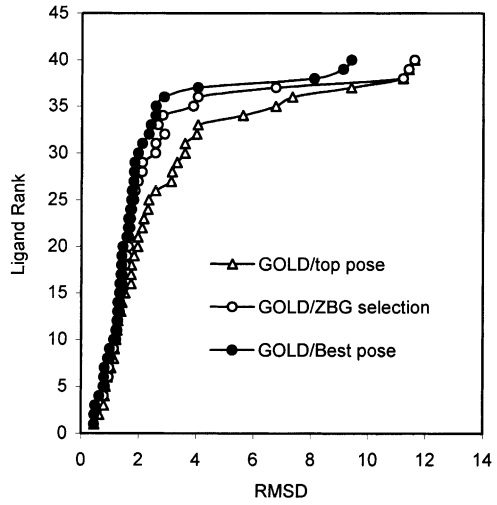

Fig. 8. Comparison of different pose selection criteria for docking accuracy by GOLD for 40 metalloproteinase ligand complexes.

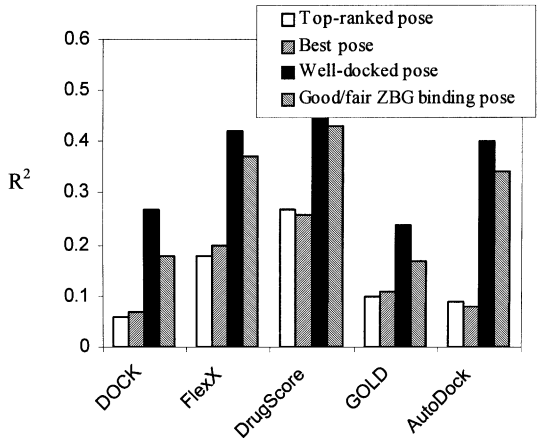

Fig. 9. Correlation between the experimental binding affinities and the calculated scores with each docking/scoring approach for different pose selection methods in the docking of 40 metalloproteinase inhibitors (Table 1).

only generated 37% of top poses with a good/fair ZBG binding.

GOLD probably provides better geometry predictions due to the use of geometrical models that guide the binding of ligands to zinc. It adopts a bifurcated tetrahedral coordination by fitting the mid-position between two coordinating electronegative atoms to imitate the bidentate binding to zinc. This feature provides better docking of hydroxarnate and carboxylate inhibitors. In contrast, the metal-ligand interactions in DOCK and AutoDock are simply modeled as electrostatic and vdW interactions with no predetermined coordination geometries. While this approach allows multiple geometries with zinc, it does not enforce correct geometry.

3.4. Selection of docking results using ZBG scoring

More than 75% of the well-docked poses were found to have good/fair ZBG binding. If the RMSD limit is increased to 2.5 Å, the percentage of the well-docked poses with good/fair ZBG binding increased to 90% for all five approaches. Only 10% of poses with good/fair ZBG binding do not dock correctly. In contrast, for poor ZBG binding, the failure rate is 95%. Obviously, proper ZBG binding is required for docking accuracy.

We therefore used ZBG scoring to re-select the best docking pose from the 30 docked solutions generated by each docking approach. The selected pose has the highest docking energy score with a good or fair ZBG score, thus eliminating any pose without appropriate ZBG binding geometry. As a result of the re-selection, the number of the well-docked poses increased to 25, 24, 18, 17, and 13 for Gold, AutoDock, DrugScore, FlexX, and DOCK, respectively. These success rates are comparable to the best pose selection and significantly better than the top-ranked selection (Table 3). Fig. 8 shows a comparison of the three sets of selected poses for GOLD docking. Promisingly, the ZBG-selected poses are almost as good as the best poses.

3.5. Scoring reliability

Fig. 9 shows the correlation between the observed binding affinities (pK_i) and the calculated scores predicted by each docking approach for the 40 metalloproteinase complexes. Four cases differing in the docked pose selection were compared. The top-ranked pose with lowest docked energies is generally used as standard selection in docking programs. However, the correlations between the observed binding affinities and the scores were poor for all five scoring functions. The best squared correlation coefficient for DrugScore was $R^2 = 0.27$ with a standard deviation (S.D.) = 1.89 log units. The reason for such poor performance of these scoring functions is most probably the presence of many wrong-docked poses among the top-ranked selections. Scoring unlikely geometries cannot be expected to predict affinity reliably. Hence, the detection of incorrectly docked poses is a crucial prerequisite for a correct estimation of binding affinities. DrugScore that was designed to find the native binding mode among docked structures [19] provided the best scoring, yet the performance was inadequate for effective virtual screening.

The use of best poses (lowest RMSD among the 30 docked solutions) minimizes incorrect docking and is expected to give the best scoring reliability. However, no improvement was observed in this case (Fig. 9). The correlations were as weak as the top-ranked case; the best approach, DrugScore, only achieved $R^2 = 0.25$. A possible explanation of this phenomenon is that there are still too many wrong-docked cases among the best poses. However, using only a subset of the best poses, the well-docked poses with an RMSD value less than 2 Å the correlation coefficients between the observed binding affinities and the calculated values increased greatly for all the scoring methods. DrugScore still provided

Table 6
Regression parameters for the subsets of metalloproteinase inhibitors[a]

Approach	Hydroxamates ($n = 13$)			Carboxylates ($n = 8$)			Phosphonates ($n = 8$)			Overall[b]		
	Slope	Intercept	R^2	Slope	Intercept	R^2	Slope	Intercept	R^2	Slope	Intercept	R^2
DOCK	−0.061 (0.015)	0.911 (1.509)	0.597 (1.540)	−0.019 (0.006)	4.611 (0.945)	0.582 (0.614)	−0.069 (0.019)	1.202 (2.254)	0.679 (1.803)	1.001 (0.129)	−0.025 (1.005)	0.689 (1.333)
FlexX	−0.188 (0.048)	2.235 (1.237)	0.588 (1.569)	−0.068 (0.027)	5.244 (0.837)	0.516 (0.662)	−0.305 (0.066)	−0.402 (2.085)	0.781 (1.493)	1.002 (0.120)	−0.004 (0.930)	0.722 (1.263)
DrugScore	−0.107 (0.024)	0.451 (1.493)	0.642 (1.463)	−0.026 (0.009)	5.150 (0.749)	0.600 (0.606)	−0.075 (0.013)	2.856 (1.152)	0.845 (1.257)	1.000 (0.105)	−0.002 (0.815)	0.772 (1.143)
GOLD	−0.030 (0.008)	0.991 (1.633)	0.556 (1.623)	−0.009 (0.006)	4.744 (1.266)	0.410 (0.731)	−0.040 (0.013)	−0.623 (3.118)	0.620 (1.960)	1.015 (0.146)	−0.087 (1.128)	0.641 (1.434)
AutoDock	−0.519 (0.123)	1.532 (1.325)	0.617 (1.513)	−0.181 (0.073)	5.111 (0.904)	0.510 (0.669)	−0.793 (0.247)	−0.328 (2.960)	0.632 (1.933)	1.000 (0.134)	−0.002 (1.038)	0.675 (1.366)
X-CSCORE	−2.581 (0.268)	−7.198 (1.472)	0.893 (0.796)	0.793 (0.165)	1.860 (1.138)	0.791 (0.432)	3.128 (0.585)	−9.823 (3.537)	0.827 (1.328)	1.000 (0.071)	−0.001 (0.558)	0.879 (0.831)

[a] The scoring results were calculated using the experimental structures of ligands in complexes. Standard deviations for the parameters are given in the parentheses beneath the parameters. The number beneath the R^2 value is the standard error in log energy units of the predicted energies.
[b] After subset re-scoring.

the best results ($R^2 = 0.46$), followed by FlexX ($R^2 = 0.42$) and AutoDock ($R^2 = 0.40$). The knowledge-based scoring function DrugScore is somewhat superior to other scoring functions for the metalloproteinases. On the other hand, the traditional force field scoring approaches perform less well in the metalloproteinase docking, probably due to the lack of appropriate force fields for zinc that accurately model the coordination metal/ligand interactions.

Interestingly, for the pose selection based on good ZBG binding, the correlations between the predicted and experimental binding affinities were almost as good as for well-docked poses. This finding is in accordance with the fact that more than 90% of good ZBG binding poses are actually well docked. As a determining factor, a good ZBG binding seems to be a necessity for the prediction of binding affinities for metalloproteinase inhibitors. Analysis of the AutoDock results showed that the ZBG binding contributes significantly to the predicted energies. For cases with good ZBG binding, the energy contributions from the zinc/ligand interactions amounted to up to 20% of the total energies. However, for poses with poor zinc binding, the share was only 1–5%.

To alleviate a generally poor description of zinc binding in scoring functions, ligands differing in ZBGs can be treated separately. In fact, the SMoG2001 scoring function predicts the binding affinities for metalloproteinases much better using the subsets of ligands with identical ZBGs than if different ZBGs were combined [20]. We investigated three subsets in our 40 metalloproteinase data set (13 hydroxamates, 8 carboxylates, and 8 phosphonates or phosphoramidates) using the five scoring approaches and reached a similar conclusion. As Table 6 shows, the scoring reliability associated within each subset improved significantly. For DrugScore, the R^2 for hydroxamates, carboxylates, and phosphonates (phosphoramidates) increased to 0.64, 0.60, and 0.85, respectively (Fig. 10). Furthermore, when the scores were calculated using the regression equations for each subset, the overall scoring reliabilities for all five approaches also improved significantly (Table 6). Differences in slopes and intercepts indicate that classification into subsets is justified.

3.6. Consensus scoring for metalloproteinase inhibitors

Consensus scoring is a widely used approach to improve the scoring reliability and hit rate in virtual screening. As

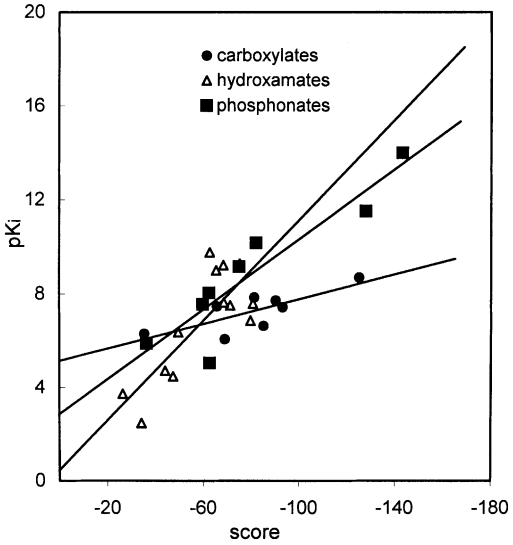

Fig. 10. Correlation between the experimental binding affinities and the calculated scores within three subsets of metalloproteinase inhibitors using DrugScore. The regression coefficients and statistical indices are summarized in Table 6.

Table 7
Correlation coefficients between the experimental affinities of 40 metalloproteinase complexes and predicted values by each individual scoring function for experimental geometries of ligand/receptor complexes. Standard error (SE) of the predicted energies in log units obtained from the regression

Scoring function	R^2	S.E.
F_Score	0.46	1.62
G_Score	0.33	1.82
PMF	0.30	1.87
D_Score	0.27	1.91
ChemScore	0.34	1.81
DrugScore	0.58	1.45
AutoDock	0.45	1.65
X-CSCORE	0.52	1.56

more scoring functions are introduced, a wise selection of the most appropriate scoring functions for a specific problem and a combination of these scoring functions have been shown to outperform one single scoring function [62–64]. We compared eight scoring functions in the prediction of binding affinities for metalloproteinase inhibitors. Five scoring functions are included in CScore [65]: F_Score is the original FlexX scoring function; D_Score and G_Score are similar to the scoring functions used in DOCK and GOLD; PMF is a knowledge-based scoring function [18]; ChemScore is an empirical scoring function [16]. Another consensus scoring function, X-CSCORE, consists of three empirical scoring functions, HPScore, HMScore, and HSScore, which use different models for the hydrophobic effects. Since the scores obtained from the three scoring functions for the metalloproteinases are very similar, we used the average value as the original paper suggested [66].

To eliminate problems in docking accuracy that could distort the evaluation of scoring reliability, the experimental structures of ligands in complexes were used to compute each score. Table 7 shows the correlations between the experimental and predicted binding affinities associated with these scoring functions for the metalloproteinases. As can be seen, performances of each single scoring function were still rather poor. The results were generally consistent with our previous observations; DrugScore performed best with $R^2 = 0.58$. However, the other knowledge-based scoring function, PMF, does not show better results than the other scoring functions.

It should be noted that although the overall performances of these scoring functions appear unsatisfactory, the scoring on the subset of metalioproteinase inhibitors showed significant improvement (Table 6). In the following virtual screening study, we selected X-CSCORE to process the docking results due to its best performance in subset prediction of binding energies. Fig. 11 shows the scoring reliability of X-CSCORE on the three subsets of metalloproteinase inhibitors. The R^2 for hydroxamate, carboxylate, and phosphonate are 0.89, 0.79, and 0.83, respectively.

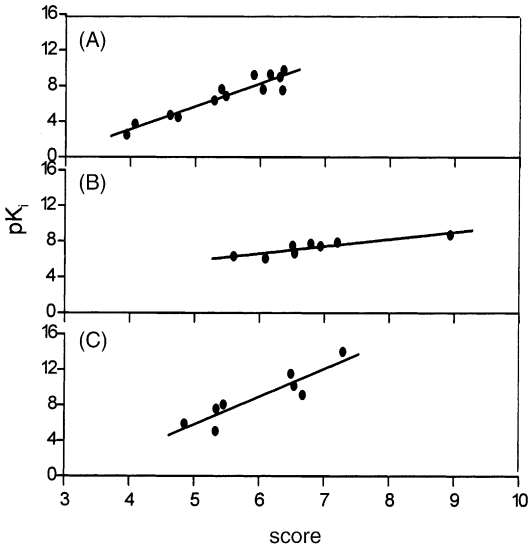

Fig. 11. Correlation between the experimental binding affinities and the calculated scores using X-CSCORE for hydroxamates (A), carboxylates (B), and phosphonates (C).

3.7. Virtual screening for metalloproteinases inhibitors

The screening of a focused MMP inhibitor library of 500 compounds with 10 known MMP inhibitors was performed on the target protein MMP-3 [40] using the default parameters as described. The screening efficiencies of the five approaches in terms of identifying the potent MMP inhibitors are depicted in Fig. 12. DrugScore is clearly best in placing the known inhibitors among the higher-ranked candidates. The hit rates among the top 5% selection are shown in Fig. 13. The hit rates associated with each docking/scoring

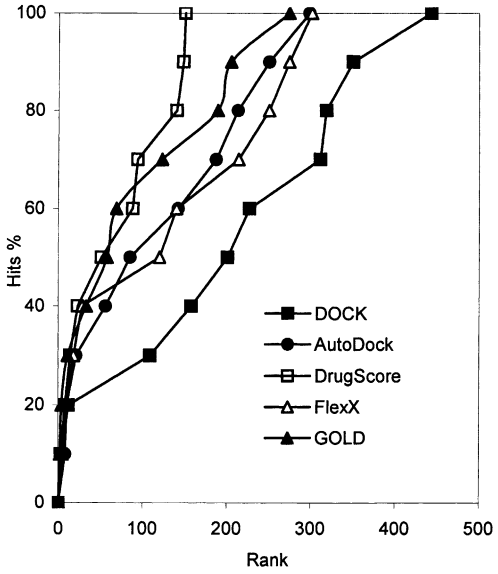

Fig. 12. Ranking of confirmed hits with the five docking/scoring approaches.

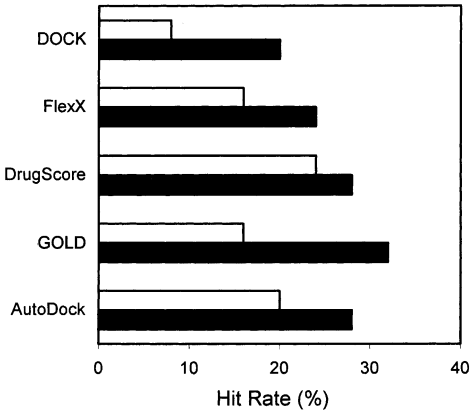

Fig. 13. Hit rates (percent of known inhibitors among 5% top selection of the total compounds) of five docking/scoring approaches for metalloproteinase inhibitors. The blank bars denote the original docking/scoring approaches, while the pattern bars denote the original docking combined ZBG scoring and subset re-scoring.

approach varied between 8 and 25%. DrugScore again was the best approach, scoring 5 out of 10 known potent inhibitors in the top 5%. Considering that most of the confirmed hits are potent inhibitors, the hit rates in real database screening (usually weak leads with K_i in micromolar range) would be expected to be much lower.

In order to improve the hit rate, we used the ZBG scoring to re-select the docking results. The compounds without ZBG binding were removed. The reduced data set was separated into subsets according to the ZBG type (hydroxamate, carboxylate, and phosphorus-containing groups). Each subset was then re-scored using X-CSCORE and the associated regression equation (Table 6). As a result of subset re-scoring, all docking programs improved significantly (Fig. 13). The best hit rate was obtained with GOLD, consistent with its better performance in the prediction of proper binding mode as well as the proper ZBG binding. Apparently, detection of the proper binding mode in docking is a critical step to improve the scoring and ranking in virtual screening.

ZBG scoring is useful as a post-docking filter to eliminate unreliable docking results. We found that 20–30% of the docked compounds lack appropriate ZBG binding and should be removed. Large molecules in particular often show up as false positives and can be removed using ZBG filtering. Elimination of the false positives improves the chances of finding appropriate hits, as clearly demonstrated in Fig. 13. Monitoring of ZBG scores also focuses the compounds identified in virtual screening and has the potential for identifying new leads.

4. Conclusions

In summary, we have compared a number of docking systems and identified those that show the greatest accuracy in positioning the ligands of zinc metalloproteinases into the active site. Several scoring systems were evaluated, and knowledge-based systems were identified as the most accurate. Proper zinc coordination geometry was shown to be a prerequisite for quality docking. The ZBG filtering provides a handy tool for re-selection of appropriate top-ranked poses. The importance of subdividing the ligands into groups based on the functionality complexed with zinc was confirmed and was particularly effective if consensus scoring was used to improve results. Finally, we demonstrated that ZBG filtering and subset re-scoring improve the hit rate and eliminate false positives that often plague virtual screening.

Acknowledgements

This work was supported by NIH NCRR (1 P20 RR15566) and (1 P20 RR 16471), and the Department of Pharmaceutical Sciences, School of Pharmacy, North Dakota State University, Fargo. The authors thank Drs. Mukund Sibi, Gregory Cook, and Peter Baricic for helpful discussions.

References

[1] I.D. Kuntz, Structure-based strategies for drug design and discovery, Science 257 (1992) 1078–1082.
[2] J. Drews, Drug discovery: a historical perspective, Science 287 (2000) 1960–1964.
[3] R.D. Taylor, P.J. Jewsbury, J.W. Essex, A review of protein-small molecule docking methods, J. Comput.-Aided Mol. Des. 16 (2002) 151–166.
[4] B. Cox, J.C. Denyer, A. Binnie, M.C. Donnelly, B. Evans, D.V. Green, J.A. Lewis, T.H. Mander, A.T. Merritt, M.J. Valler, S.P. Watson, Application of high-throughput screening techniques to drug discovery, Prog. Med. Chem. 37 (2000) 83–133.
[5] I.D. Kuntz, J.M. Blaney, S.J. Oatley, R. Langridge, T.E. Ferrin, A geometric approach to macromolecule-ligand interactions, J. Mol. Biol. 161 (1982) 269–288.
[6] J.A.E. Todd, S.A. Makino, G. Skillman, I.D. Kuntz, DOCK 4.0: Search strategies for automated molecular docking of flexible molecule databases, J. Comput.-Aided Mol. Des. 15 (2001) 411–428.
[7] D.S. Goodsell, A.J. Olson, Automated docking of substrates to proteins by simulated annealing, Proteins 8 (1990) 195–202.
[8] M. Rarey, B. Kramer, T. Lengauer, G. Klebe, A fast flexible docking method using an incremental construction algorithm, J. Mol. Biol. 261 (1996) 470–489.
[9] W. Welch, J. Ruppert, A.N. Jain, Hammerhead: fast, full automated docking of flexible ligands to protein binding sites, Chem. Biol. 3 (1996) 449–462.
[10] D.S. Goodsell, G.M. Morris, A.J. Olson, Docking of flexible ligands: applications of AutoDock, J. Mol. Recognition 9 (1996) 1–5.
[11] G.M. Morris, D.S. Goodsell, R.S. Halliday, R. Huey, W.E. Hart, R.K. Belew, A.J. Olson, Automated docking using a Lamarckian genetic algorithm and empirical binding free energy function, J. Comput. Chem. 19 (1998) 1639–1662.
[12] G. Jones, P. Wilett, R.C. Glen, A.R. Leach, R. Taylor, Development and validation of a genetic algorithm for flexible docking, J. Mol. Biol. 267 (1997) 727–748.
[13] C. McMartin, R.S. Bohacek, QXP: powerful, rapid computer algorithms for structure-based drug design, J. Comput.-Aided Mol. Des. 11 (1997) 333–344.

[14] C.A. Baxter, C.W. Murray, D.E. Clark, D.R. Westhead, M.D. Eldridge, Flexible docking using Tabu search and an empirical estimate of binding affinity, Proteins 33 (1998) 367–382.
[15] H.J. Böhm, Prediction of binding constants of protein ligands: a fast method for the priorization of hits obtained from de novo design or 3D database search programs, J. Comput.-Aided. Mol. Des. 12 (1998) 309–323.
[16] M.D. Eldridge, C.W. Murray, T.R. Auton, G.V. Paolini, R.P. Mee, Empirical scoring functions: I. The development of a fast empirical scoring function to estimate the binding affinity of ligands in receptor complexes, J. Comput.-Aided Mol. Des. 11 (1997) 425–445.
[17] R. Wang, L. Liu, L. Lai, Y. Tang, SCORE: a new empirical method for estimating the binding affinity of a protein–ligand complex, J. Mol. Model 4 (1998) 379–394.
[18] I. Muegge, Y.C. Martin, A general and fast scoring function for protein–ligand interactions: a simplified potential approach, J. Med. Chem. 42 (1999) 791–804.
[19] H. Gohlke, M. Hendlich, G. Klebe, Knowledge-based scoring function to predict protein–ligand interactions, J. Mol. Biol. 295 (2000) 337–356.
[20] A.V. Ishchenko, E.I. Shakllnovich, SMall Molecule Growth 2001 (SMoG2001): an improved knowledge-based scoring function for protein–ligand interactions, J. Med. Chem. 45 (2002) 2770–2780.
[21] M. Vieth, J.D. Hirst, A. Kolinski, C.L. Brooks III, Assessing energy functions for flexible docking, J. Comput. Chem. 19 (1998) 1612–1622.
[22] M. Stahl, M. Rarey, Detailed analysis of scoring functions for virtual screening, J. Med. Chem. 44 (2001) 1035–1042.
[23] D. Leung, G. Abbenante, D.P. Fairlie, Protease inhibitors: current status and future prospects, J. Med. Chem. 43 (2000) 305–341.
[24] H. Matter, W. Schwab, D. Barbier, G. Billen, B. Haase, B. Neises, M. Schudok, W. Thorwart, H. Schreuder, V. Brachvogel, P. Lonze, K.U. Weithmann, Quantitative structure-activity relationship of human neutrophil collagenase (MMP-8) inhibitors using comparative molecular field analysis and X-ray structure analysis, J. Med. Chem. 42 (1999) 1908–1920.
[25] R. Kiyama, Y. Tamura, F. Watanabe, H. Tsuzuki, M. Ohtani, M. Yodo, Homology modeling of gelatinase catalytic domains and docking simulations of novel sulfonamide inhibitors, J. Med. Chem. 42 (1999) 1723–1738.
[26] J.M. Chen, F.C. Nelson, J.I. Levin, D. Mobiho, F.J. Moy, R. Nilakantan, A. Zask, R. Powers, Structure-based design of a novel, potent, and selective inhibitor for MMP- 13 utilizing NMR spectroscopy and computer-aided molecular design, J. Am. Chem. Soc. 122 (2000) 9648–9654.
[27] S. Ha, R. Andreani, A.R.I. Muegge, Evaluation of docking/scoring approaches: a comparative study based on MMP3 inhibitors, J. Comput.-Aided Mol. Des. 14 (2000) 435–448.
[28] S. Hanessian, N. Moitessier, E. Therrien, A comparative docking study and the design of potentially selective MMP inhibitors, J. Comput.-Aided Mol. Des. 15 (2001) 873–881.
[29] O.A.T. Donini, P.A. Kollman, Calculation and prediction of binding free energies for the matrix metalloproteinases, J. Med. Chem. 43 (1999) 4180–4188.
[30] O.V. Buzko, A.C. Bishop, K.M. Shokat, Modified AutoDock for accurate docking of protein kinase inhibitors, J. Comput.-Aided Mol. Des. 16 (2002) 113–127.
[31] E. Perola, K. Xu, T.M. Kollmeyer, S.H. Kaufmann, F.G. Prendergast, Y.-P. Pang, Successful virtual screening of a chemical database for farnesyltransferase inhibitor leads, J. Med. Chem. 43 (2000) 401–408.
[32] Y.-P. Pang, E. Perola, K. Xu, F.G. Prendergast, EUDOC: a computer program for identification of drug interaction sites in macromolecules and drug leads from chemical databases, J. Comput. Chem. 22 (2001) 1750–1771.
[33] M.L. Verdonk, J.C. Cole, R. Taylor, SuperStar: a knowledge-based approach for identifying interaction sites in proteins, J. Mol. Biol. 289 (1999) 1093–1108.
[34] A.E. Yu, R.E. Hewitt, E.W. Connor, W.G. Stetler-Stevenson, Matrix metalloproteinases: novel targets for directed cancer therapy, Drugs Aging 11 (1997) 229–244.
[35] M.J. Wyvratt, A.A. Patchett, Recent developments in the design of angiotensin-converting enzyme inhibitors, Med. Res. Rev. 5 (1985) 483–531.
[36] H.M. Berman, J. Westbrook, Z. Feng, G. Gilliland, T.N. Bhat, H. Weissig, I.N. Shindyalov, P.E. Bourne, The Protein Data Bank, Nucl. Acids Res. 28 (2000) 235–242.
[37] B. Lovejoy, A.R. Welch, S. Carr, C. Luong, C. Broka, R.T. Hendricks, J.A. Campbell, K.A. Walker, R. Martin, H. Van Wart, M.F. Browner, Crystal structures of mmp-1 and- 13 reveal the structural basis for selectivity of coilagenase inhibitors, Nat. Struct. Biol. 6 (1999) 217–221.
[38] A.G. Pavlovsky, M.G. Williams, Q.Z. Ye, D.F. Ortwine, C.F. Purchase II, A.D. White, V. Dhanaraj, B.D. Roth, L.L. Johnson, D. Hupe, C. Humblet, T.L. Blundell, X-ray structure of human stromelysin catalytic domain complexed with non-peptide inhibitors: implications for inhibitor selectivity, Protein Sci. 8 (1999) 1455–1462.
[39] J.W. Becker, A.I. Marcy, L.L. Rokosz, M.G. Axel, J.J. Burbaum, P.M. Fitzgerald, P.M. Cameron, C.K. Esser, W.K. Hagmann, J.D. Hermes, Stromelysin-1: three-dimensional structure of the inhibited catalytic domain and of the C-truncated proenzyme, Protein Sci. 4 (1995) 1966–1976.
[40] C.K. Esser, R.L. Bugiansi, C.G. Caldwell, K.T. Chapman, P.L. Durette, N.N. Girotra, I.E. Kopka, T.J. Lanza, D.A. Levorse, M. MacCoss, K.A. Owens, M.M. Ponpipom, J.P. Simeone, R.K. Harrison, L. Niedzwiecki, J.W. Becker, A.I. Marcy, M.G. Axel, A.J. Christen, J. McDonnell, V.L. Moore, J.M. Olszewski, C. Saphos, D.M. Visco, F. Shen, A. Colletti, P.A. Krieter, W.K. Hagmami, Inhibition of stromelysin-1 (MMP-3) by P1′-biphenylethyl carboxyalkyl dipeptides, J. Med. Chem. 40 (1997) 1026–1040.
[41] B.C. Finzel, E.T. Baldwin, G.L. Bryant, G.F. Hess, J.W. Wilks, C.M. Trepod, J.E. Mott, V.P. Marshall, G.L. Petzold, R.A. Poorman, T.L. O'Sullivan, H.J. Schostarez, M.A. Mitchell, Structural characterizations of nonpeptidic thiadiazole inhibitors of matrix metalloproteinases reveal the basis for stromelysin selectivity, Protein Sci. 7 (1998) 2118–2126.
[42] M.F. Browner, W.W. Smith, A.L. Castelhano, Matrilysin-inhibitor complexes: common themes among metalloproteases, Biochemistry 34 (1995) 6602–6610.
[43] F. Grams, M. Crimmin, L. Hinnes, P. Huxley, M. Pieper, H. Tschesche, W. Bode, Structure determination and analysis of human neutrophil coliagenase complexed with a hydroxamate inhibitor, Biochemistry 34 (1995) 14012–14020.
[44] F. Grams, P. Reinemer, J.C. Powers, T. Kleine, M. Pieper, H. Tschesche, R. Huber, W. Bode, X-ray structures of human neutrophil collagenase complexed with peptide hydroxamate and peptide thiol inhibitors. Implications for substrate binding and rational drug design, Eur. J. Biochem. 228 (1995) 830–841.
[45] H. Brandsteffer, R.A. Engh, E.G. Von Roedem, L. Moroder, R. Huber, W. Bode, F. Grams, Structure of malonic acid-based inhibitors bound to human neutrophil collagenase. A new binding mode explains apparently anomalous data, Protein Sci. 7 (1998) 1303–1309.
[46] T. Stams, J.C. Spurlino, D.L. Smith, R.C. Wahi, T.F. Ho, M.W. Qoronfleh, T.M. Banks, B. Rubin, Structure of human neutrophil collagenase reveals large S1′ specificity pocket, Nat. Struct. Biol. 1 (1994) 119–123.
[47] W. Bode, P. Reinemer, R. Huber, T. Kleine, S. Schnierer, H. Tschesche, The X-ray crystal structure of the catalytic domain of human neutrophil collagenase inhibited by a substrate analogue reveals the essentials for catalysis and specificity, EMBO J. 13 (1994) 1263–1269.
[48] B.W. Matthews, Structural basis of the action of thermolysin and related zinc peptidases, Acc. Chem. Res. 21 (1988) 333–340.
[49] J.F. Gaucher, M. Selkti, G. Tiraboschi, T. Prange, B.P. Roques, A. Tomas, M.C. Foumie-Zaluski, Crystal structures

of alpha-mercaptoacyldipeptides in the thermolysin active site: structural parameters for a Zn monodentation or bidentation in metalloendopeptidases, Biochemistry 38 (1999) 12569–12576.
[50] S. Mangani, P. Carloni, P. Orioli, Crystal structure of the complex between carboxypeptidase A and the biproduct analog inhibitor L-benzylsuccinate at 2.0 Å resolution, J. Mol. Biol. 223 (1992) 573–578.
[51] A.M. Cappalonga, R.S. Alexander, D.W. Christianson, Structural comparison of sulfodumine and sulfonamide inhibitors in their complexes with zinc enzymes, J. Biol. Chem. 267 (1992) 19192–19197.
[52] A. Teplyakov, K.S. Wilson, P. Orioli, S. Mangani, High-resolution structure of the complex between carboxypeptidase-A and L-phenyl lactate, Acta Cryst. D49 (1993) 534–540.
[53] D.W. Christianson, W.N. Lipscomb, X-ray crystallographic investigation of substrate binding to carboxypeptidase A at subzero temperature, Proc. Natl. Acad. Sci. U.S.A. 83 (1986) 7568–7572.
[54] H. Kim, W.N. Lipscomb, Crystal structure of the complex of carboxypeptidase A with a strongly bound phosphonate in a new crystalline form: comparison with structures of other complexes, Biochemistry 29 (1990) 5546–5555.
[55] H. Kim, W.N. Lipscomb, Comparison of the structures of three carboxypeptidase A-phosphonate complexes determined by X-ray crystallography, Biochemistry 30 (1991) 8171–8180.
[56] SYBYL Molecular Modeling Software, v6.8; Tripos Associates, St. Louis, MO.
[57] J. Gasteiger, M. Marsili, Iterative partial equalization of orbital electronegativity. A rapid access to atomic charges, Tetrahedron 36 (1980) 3219–3228.
[58] M.L. Connolly, Solvent accessible surfaces of proteins and nucleic acids, Science 221 (1983) 4612–4615.
[59] G.M. Verkhivker, D. Bouzida, D.K. Gehlhaar, P.A. Rejto, S. Arthurs, A.B. Colson, S.T. Freer, V. Larson, B.A. Luty, T. Marrone, P.W. Rose, Deciphering common failures in molecular docking of ligand–protein complexes, J. Comput.-Aided Mol. Des. 14 (2000) 731–751.
[60] I.L. Alberts, K. Nadassy, S.J. Wodak, Analysis of zinc binding sites in protein crystal structures, Protein Sci. 7 (1998) 1700–1716.
[61] F. Cheng, R. Zhang, X. Luo, J. Shen, X. Li, J. Gu, W. Zhu, J. Shen, I. Sagi, R. Ji, K. Chen, H. Jiang, Quantum chemistry study on the interaction of the exogenous ligands and the catalytic zinc ion in matrix metalloproteinases, J. Phys. Chem. (B) 106 (2002) 4552–4559.
[62] P.S. Charifson, J.J. Corkery, M.A. Murcko, W.P. Walters, Consensus scoring: a method for obtaining improved hit-rates from docking databases of three-dimensional structures into proteins, J. Med. Chem. 42 (1999) 5100–5109.
[63] C. Bissantz, G. Folkers, D. Rognan, Protein-based virtual screening of chemical databases. 1. Evaluation of different docking/scoring combinations, J. Med. Chem. 43 (2000) 4759–4767.
[64] G.E. Terp, B.N. Johansen, I.T. Christensen, F.S. Jorgensen, A new concept for multidimensional selection of ligand conformations (MultiSelect) and multidimensional scoring (MultiScore) of protein-ligand binding affinities, J. Med. Chem. 44 (2001) 2333–2343.
[65] R.D. Clark, A. Strizhev, J.M. Leonard, J.F. Blake, J.B. Matthew, Consensus scoring for ligand/protein interactions, J. Mol. Graph. Modeling 20 (2002) 281–295.
[66] R. Wang, L. Lai, S. Wang, Further development and validation of empirical scoring functions for structure-based binding affinity prediction, J. Comput.-Aided Mol. Des. 16 (2002) 11–26.